Seasonal Variability of PM_{10} Chemical Composition Including 1,3,5-triphenylbenzene, Marker of Plastic Combustion and Toxicity in Wadowice, South Poland

Przemysław Furman[1], Katarzyna Styszko[2*], Alicja Skiba[1], Damian Zięba[1], Mirosław Zimnoch[1], Magdalena Kistler[3], Anne Kasper-Giebl[3], Stefania Gilardoni[4]

[1] AGH University of Science and Technology, Faculty of Physics and Applied Computer Science, Department of Applied Nuclear Physics, Krakow, Poland

[2] AGH University, Faculty of Energy and Fuels, Department of Coal Chemistry and Environmental Sciences, Krakow, Poland

[3] TU Wien, Institute of Chemical Technologies and Analytics, Vienna, Austria

[4] Institute of Polar Sciences-National Research Council, Bologna, Italy

Abstract

The objective of this research was to evaluate the seasonal variation of the chemical composition of PM_{10} including polycyclic aromatic hydrocarbons (PAHs) and 1,3,5-triphenylbenzene (135TPB), which is a well known marker of plastic combustion. The presented work is a part of the project concerning assessment of air quality of small cities around Krakow agglomeration. Monitoring campaign was conducted between February and October 2017 in Wadowice, a small city in Krakow agglomeration, South Poland. To widen the knowledge of Krakow's agglomeration air quality, other aerosol chemical components were analyzed. Ion chromatography (IC) was used for analysis of cations and anions, while gas chromatography-mass spectrometry (GC-MS) was used for PAHs. Samples were also analyzed for OC/EC (organic/elemental carbon) by thermal-optical analysis with a Sunset Laboratory carbon analyzer, Sunset Inc. The co-combustion of plastic in addition to conventional fuels and the respective impact on air quality is evaluated via the concentration of the marker compound 135TPB. Co-combustion of plastics with fuels resulted in a higher abundance of fluorene and most of 4-6 ring PAHs, in agreement with recent literature. Authors proved that other sources besides plastic burning, including road transport, residential heating, residential combustion, industrial emissions, affect the air quality in South Poland. The modeling tool Hybrid Single-Particle Lagrangian Integrated Trajectory model (HYSPLIT), developed by NOAA's Air Resources Laboratory, was used to define the possible areas outside Wadowice contributing to urban air pollution.

Keywords: atmospheric aerosols, PAHs, 1,3,5-triphenylbenzene, ions, OC/EC

*Corresponding author. Tel: +48 12 6172032; Fax: +48 12 6172399

E-*mail address*: styszko@agh.edu.pl

INTRODUCTION

Particulate matter is a complex mixture of different chemical compounds, including nitrates, sulphates, as well as elemental and organic carbon (OC, EC). Some components of organic carbon are particularly toxic, such as polycyclic aromatic hydrocarbons (PAHs) and their derivatives (nitro-PAHs, hydroxy-PAHs). Particulate matter origin can be both natural and anthropogenic. Anthropogenic sources include, above all, solid fuel combustion processes, transport and illegal waste incineration processes (Putaud *et al*., 2010). At the urban site, coal is used in ca. 50% of households for residential heating purposes (Lochno *et al*., 2013; Styszko *et al*., 2015). Over the last few decades, concern about the health effects has grown, mainly due to the occurrence of increasingly high concentrations of particulate matter in the atmosphere. In Poland, the daily concentration limit of PM_{10} is 50 μg m^{-3}, the daily level alert is set to100 μg m^{-3}, whereas the daily level alarm is 150 μg m^{-3}. The limits of annual average concentrations of PM_{10} and $PM_{2.5}$ are 40 μg m^{-3} and 25 μg m^{-3}, respectively.

Carbonaceous aerosols (CA) constitute a major fraction of particulate matter (PM) present in urban atmospheres. Their contribution varies, depending on the location, between ca. 30 and 40% of the total mass of coarse fraction (PM_{10} minus $PM_{2.5}$) (Szramowiat *et al.*, 2016), and between ca. 10 and 50% of the total particulate matter (PM_{10}) (Querol *et al*., 2013). Carbonaceous fraction of PM is a complex mixture of different compounds, that can be grouped into elemental carbon (EC), organic carbon (OC) and carbonate or mineral carbon (CC). Organic carbon (OC) accounts for a large fraction of atmospheric aerosol and its molecular composition might change during

atmospheric processesing and aging. The ratio of OC to EC is an important index that reflects the source type and strength (Ji *et al*., 2016), as well as atmospheric processing. As indicated in the literature (Liu *et al*., 2016; Samara *et al*., 2014; Sillanpää *et al*., 2006) a low OC/EC ratio can be associated with fresh traffic aerosol (1.7-2.3 and 0.5-0.8 for light-duty gasoline and heavy duty diesel vehicles, respectively) (Na *et al*., 2004; Pio *et al*., 2011; Samara *et al*., 2014), whereas higher ratios are observed in residential heating emissions or in areas dominated by secondary organic aerosol (SOA). Examples of OC/EC ratios are 4.2 for wood combustion and 12.7 for natural gas (Na *et al*., 2004), while Zhang *et al*. (2013) showed that emissions from fireplaces/woodstoves can vary from (2.8-7.5) to relatively high values (26-119) (Na *et al*., 2004; Zhang *et al*., 2013). Tian *et al*. reported the average OC/EC ratio for coal (1.4 ± 1.3 and 6.3 ± 1.3 for bituminous and anthracite, respectively) whereas agricultural biomass burning ratio was 13.7 ± 2.7 (Tian *et al*., 2017). Since SOA formation contributes exclusively to OC concentration, SOA dominated environments show generally OC/EC ratios larger than 4 (Sandrini *et al*., 2014; Zeng *et al*., 2011).

Polycyclic aromatic hydrocarbons (PAHs) are one of the many particulate matter components. A significant increase of PAHs in the atmosphere has a negative impact on the environment and human health. PAHs have mutagenic and carcinogenic effects (Kozielska *et al*., 2015; Kuskowska *et al*., 2018; Rogula-Kozłowska *et al*., 2018, 2013). The strongest carcinogenic compounds are benzo[a]pyrene and dibenzo[a,h]anthracene. Although aerosol health outcomes depend on different factors, including personal exposure and sensitivity, it is important to highlight that PAHs are present in smaller and inhalable aerosol particles, and enter the human body reaching the

alveolar ephitelium. Thus, they are potentially serious threat for human health. (Ciecierska and Obiedziński, 2012; Kubiak, 2013; Parol *et al*., 2014). The biggest impact is observed at the location of their absorption into the body (Kubiak, 2013). Only the target value (1 ng m^{-3}) for benzo[a]pyrene in the air is specified by the legislation (DIRECTIVE 2004/107/EC), since benzo[a]pyrene is considered a representative substance for the PAHs group. This value is a marker of the carcinogenic risk set out in the Regulation of the Minister of the Environment of Poland from 13 September 2012 on setting limit values of substances in the air (Dz.U. 2012 nr 0 poz. 1032) (Pachurka *et al*., 2014). Agency for Toxic Substances and Disease Registry classified 17 PAHs as the most dangerous in terms of potential exposure and adverse impact on human health, while the Environmental Protection Agency (EPA) compiled a list of 16 of them, which are treated as the most toxic. This group includes: acenaphten, acenaphthylene, antracene, benzo[a]anthracene, benzo[a]pyrene, benzo[b]fluoranthene, benzo[ghi]perylene, benzo[k]fluoranthene, chrysene, dibenzo[a,h]anthracene, fluoranthene, fluorene, indeno[1,2,3-cd]pyrene, phenanthrene, pyrene, and naphthalene (EPA).

Based on previous research (Simoneit, 2015), it is urgent to include triphenylbenzene into the group of toxic and tracked PAHs, as it was proved to be promising marker for plastic and landfills burning emission. There are three possible isomers of triphenylbenzen $C_{24}H_{18}$: 1,2,3-triphenylbenzene, 1,3,5-triphenylbenzene, 1,2,4-triphenylbenzene. 1,3,5-triphenylbenzene (135TPB) is typically predominant compound, 1,2,4-triphenylbenzene usually present as a minor compound (Simoneit, 2015).

According to Simoneit et al. (2005) from the source emission test based on plastic bags (polyethylene), 63 μg triphenylbenzene per 1 g of smoke were emitted and during the same test with roadside plastic trash 208 μg g^{-1} were emitted (Simoneit *et al*., 2005). Conversely, the tests conducted in the ambient air in Sapporo (Japan) and Gosan Island (Korea) in 2001 showed that 1 g of smoke contains 22 μg and 12 μg of triphenylbenzene, respectively (Simoneit *et al*., 2004).

In Poland, the problem of high particulate matter concentration is particularly evident in the Malopolska, where the high concentrations of PM are due to the terrain landform, the weather conditions, as well as the presence of large industrial plants emitting pollution directly into the atmosphere (Skiba *et al*., 2019; Styszko *et al*., 2019a; Styszko *et al*., 2019b). The highest concentration values are observed in winter, where the PM_{10} limit (50 μg m^{-3}-daily) is significantly exceeded each year. Majority of the households, located in suburban and rural areas are heated individually by solid fuels combustion in manually operated boilers, often with low efficiency. In Poland and Czech Republic a new regulation has been adopted to allow environmental inspectors to break privacy and to control the solid combustion byproducts, to inspect burning residues in boilers. Thus, monitoring of 1,3,5-triphenylbenzene (135TPB) has been suggested as a suitable marker tracing burning of the polyethylene plastics (Furman *et al*., 2019a; Furman *et al*., 2019b, Tomsej *et al*., 2018).

The objective of this study is to characterize the chemical composition of atmospheric particulate matter (PM_{10}) and quantify their contributions in the atmosphere of small city, strongly affected by individual residential boilers, as well as industrial emissions (during different seasons).

Specific aims of the study are to determine the concentrations of 16 PAHs, 135TPB, ions and OC/EC in particulate matter. This is the first investigation in Poland on the occurrence of 135TPB in atmospheric aerosols in ambient air.

MATERIALS AND METHODS

Sampling site

PM_{10} samples were collected in the city center of Wadowice (49°88′ N 19°49′ E, 273 m n.p.m), from February to October 2017. Sampling was conducted during a pilot study characterizing air quality at sites not yet included within the routine air quality network. Due to the limited time period only part of the heating period could be sampled and even higher concentrations might be expected during the remaining months. In total, 82 PM_{10} samples during heating season (HS, February-April and October) and 72 samples during non-heating season (NHS, May-September) were collected. Wadowice city is located in southern Poland, in Malopolska voivodeship, near to the biggest city of the region-Kraków (771,069 inhabitants). Sampling site is shown in Fig. 1. The population of Wadowice is about 19,000 inhabitants with population density of about 1800 people per sq. km. Each year the city is visited by about 300,000 tourists. Air quality of the sampling area is affected by numerous small coal-fired, low efficiency boilers distributed over the city and the traffic through the city.

PM_{10} samples were collected using a low-volume sampler PNS-15 on quartz fiber filters (Whatman QM-A 47 mm diameter) with 24 h resolution. All quartz fiber filters had been preheated

for 6 h at 550 ± 8℃ and then kept at temperature 20 ± 1℃ and relative humidity 50 ± 5% for at least 24 h prior to weighting and sampling. After sampling, all filters were conditioned for 48 h, weighted with a microbalance (A&D HM-202-EC) up to accuracy of 0.01 mg, and then stored in a freezer at -20℃ until analysis. The masses of the filters before and after sampling were obtained as the average of three measurements (PN-EN 12341:2006a; PN-EN 14907:2006b).The meteorological data used in the study (air temperature, wind speed and direction, pressure and precipitation volume) were obtained from the platform: *https://www.ekologia.pl/pogoda/polska/malopolskie/wadowice/archiwum* and form the data collected by IMGW-PIB (Institute of Meteorology and Water Management): https://dane.imgw.pl/. Details on the meteorological conditions during the study period are summarized in Table 1.

CHEMICAL ANALYSES

Analysis of carbonaceous fraction

Circular punches with 1 cm diameter were analyze to measure the concentration of organic and elemental carbon by the thermal-optical method using the Sunset Laboratory OCEC Lab Aerosol Analyzer and the EUSAAR2 (European Supersites for Atmospheric Aerosol Research) protocol (Cavalli *et al*., 2010).

Accuracy and repeatability of results were regularly controlled on the basis of the determination of a sucrose solution containing 50 µg of carbon in 10 µL or by using reference filters. Limits of detection for OC and EC were equal to 0.30 µg m^{-3} and 0.015 µg m^{-3}, respectively.

Inorganic ions analysi

Concentrations of inorganic anions and cations (NO_3^-, Cl^-, SO_4^{2-}, PO_4^{3-}, Na^+, K^+, Mg^{2+}, Ca^{2+}, NH_4^+) were analyzed with isocratic ion chromatography: two circular punches (ø 8 mm) per filter were extracted under ultrasonic agitation for 40 min, in either 1.5 mL of extra pure water (anions) or in 1.5 mL of the 12 mM methane sulfonic acid (MSA) (cations), in order to determine concentrations of anions and cations, respectively.

Ion chromatography (IC) analysis was performed with a ICS-1100 instrument (Thermo Scientific), equipped with an autosampler AS-DV and ion-exchange columns:

- Ion Pac AS22 (4 x 250 mm) for anions, mobile phase: 4.5 mM Na_2CO_3 + 1.4 mM $NaHCO_3$,
- CS16 (5 x 250 mm) for cations, mobile phase: 12 mM MSA.

After electrochemical suppression (AERS 500-4 mm and CERS 500-4 mm suppressors), quantification was achieved with a conductivity detector (injection volume 25 µL, flow rate 1.2 mL min^{-1}).

Calibration was performed against external standards diluted from stock solutions supplied by VWR. The limit of detection (defined as 3 * standard deviation for the field blank samples) of the method for atmospheric samples is presented in a previous publication (Samek *et al*., 2018).

Analysis of PAHs and 135TPB

The standards of known concentration EPA 525 PAH Mix A (Sigma Aldrich) were used for the calibration of Thermo Scientific GC Trace 1310 gas chromatograph coupled with a ITQ 900 ion trap mass spectrometer and a TriPlus RSH auto-sampler. The mixture contained 16 PAHs in cyclohexane: acenaphtene (Acn), acenaphthylene (Acy), anthracene (Ant), benzo[b]fluoranthene

(BbF), benzo[a]anthracene (BaA), benzo[a]pyrene (BaP), benzo[ghi]perylene (BghiP), benzo[k]fluoranthene (BkF), chrysene (Chry), dibenzo[ah]anthracene (DahA), fluoranthene (Flt), fluorene (Flu), indeno[1,2,3-cd]pyrene (IP), naphthalene (Nap), and phenanthrene (Phen) and pyrene (Pyr). 1,3,5- triphenylbenzene (135TPB) and deuterium-labelled PAH, benzo[a]pyrene-d12 (d12-BaP, 98%) were also provided by Sigma-Aldrich (St. Louis, USA). Organic solvents, dichloromethane, cyclohexane, both for GC analysis, were purchased from Avantor Performance Materials Poland S.A.

The isolation and enrichment of PAHs and 135TPB from the filters were performed using solvent extraction. In the first stage, a punch with 22 mm diameter was cut from each filter. In non-heating season, due to low concentration of PM and to obtain concentrations of PAHs above MQL, punches of multiple filters were joined to obtain mean, weekly samples. The individual punch or ensamble of punches were placed in separate vials (20 mL) and flooded with a mixture consisting of 100 µl of internal standard (benzo[a]pyrene D12, 0.50 µg ml^{-1}) and left under hood for 20 min in order to evaporate the organic solvent. Following, samples were extracted twice with 3 ml of dichloromethane and 2 ml of cyclohexane for 40 min, using a horizontal shaker at 50 rpm. The volume of combined extracts was reduced to 250 µL in a thermoblock (AccuBlock Digital Dry Bath Labnet, Woodbridge, USA), using gentle stream of argon at 35℃. The extract were centrifuged (12,000 rpm) to separate the solid impurities that separated during the reduction of the extract volume. At the end, the concentrates (50 µL) were transferred into chromatographic vials and analysed with GC/MS/MS. The flow of helium through a GC column was constant and set at 1

203 mL min^{-1}. The programmable temperature of the vaporization injector was maintained at 250℃,
204 the transfer line at 250℃ and the ion source at 250℃. The injector was operated at splitless
205 conditions for 2 min, then turned to the split mode at the ratio of 50:1. Volume of injections was 1
206 µL. Separations was performed on a Rxi® -5Sil MS capillary column from Restek that had 30 m x
207 0.25 mm inner diameter and film thickness of 0.50 µm (5% diphenyl/ 95% dimethylpolysiloxane).
208 The temperature program for PAHs analysis was as follows: 70℃ for 2 min, from 70℃ to 150℃ at
209 20℃ min^{-1}, to 300℃ at 10℃ min^{-1}, and finally 13 min at 300℃.
210 The analyses were performed in positive mode, with electron impact ionization at 70 eV and
211 250 µA emission current. Helium (99.999%) was used as a carrier gas at 0.3 mL min^{-1}. Mass
212 spectrometry analyses was performed in the multiple reaction monitoring (MRM) mode detecting
213 the fragmentation of the precursor ions. The choice of fragmentation products for each substance
214 was based on the most intense signal. For the acquisition of the MRM transitions the analytical run
215 was split into time windows considering the expected retention time of the selected compounds.
216 Data were collected, analysed and processes using Xcalibur® software.
217 Specific and intense product ions of each target analyte were used for quantification and a
218 secondary product ion was used as qualifier ion for confirmatory purposes. The retention times,
219 characteristic ions of tested analytes and validation parameters of the method are shown in Table 2.
220 Data quality was determined based on limits of detection (LOD), limits of quantification (LOQ),
221 and the linearity of the calibration line that was estimated by analyzing the 7 points calibration
222 curves (6-7500 ng mL^{-1} for PAHs and 5-5600 ng mL^{-1} for 135TPB). The calibration curves of all

the organic compounds were highly linear ($0.994 < R^2 > 0.999$). Per-deuterated benzo[a]pyrene d12-BaP was also added to each level of standards as an internal standard to account for components losses due to volatilization or instrument bias in standards. For further quality assurance, known amount of mixed standards were spiked on blank filters and analyzed in the same steps as samples. Blank samples analysis showed none of the PAHs and 135TPB of interest. The percent recoveries for all the target compounds were in the range of 78-95%. Recoveries corrections were made to the measured concentrations. The accuracy of 95% was determined by the error obtained between the mean values of replicates of the standard solution 10 ng mL^{-1} taken as reference. The precision of 5% was calculated be means of percent relative standard deviation (% RSD).

RESULTS AND DISCUSSION

Concentrations and chemical composition of PM_{10}

The mass concentrations of PM_{10} collected during the heating season (HS, February-April and October) were higher than during non-heating season (NHS, May-September), as expected. The average PM_{10} HS concentrations was 43.3 µg m^{-3}, while the average NHS concentration was 27.1 µg m^{-3}. PM_{10} concentrations during HS varied between 10.9 and 116.8 µg m^{-3} and the range between the lowest and highest concentration was lowerin the NHS (10.8-53.7 µg m^{-3}). The highest concentration in the NHS season was noted in September. The variation of PM_{10} concentrations is reported in the Fig. 2.

Mean concentrations of PM_{10} chemical components during HS and NHS are listed in the Table 3. The analysed components accounted on average for 81% and 88% for the NHS and HS PM_{10} mass, respectively. Carbonaceous fraction (basen on organic and elemental carbon, OC+EC and the conversion of OC to organic matter (OM) as explained later) accounted for the highest share in both NHS (36%) and HS (42%) PM_{10} mass. The average contribution of inorganic ions varied from 34% to 42%, in HS and NHS, respectively, while the absolute sum of concentrations were 15 µg m^{-3} and 12 µg m^{-3}. The highest concentration was observed for Na^+ among cations and SO_4^{2-} among anions. It should be noted that average concentrations of SO_4^{2-} was similar in HS and NHS, 5.6 µg m^{-3} and 5.3 µg m^{-3}, respectively. However, average concentrations of NO_3^- and Cl^-, were up to 3 times higher in HS in comparison to NHS, due to the lower ambient temperatures that avoid ammonium nitrate volatilization.

Chemical mass closure

Chemical characterization of the main components of aerosols showed that carbonaceous components and inorganic ions exhibited the highest share in the collected aerosols, in both seasons. Similarly, Fig. 3. shows the chemical composition of PM_{10} collected in Wadowice in form of chemical mass balance. Organic matter (OM) mass, i.e. the mass of organic carbon and the associated heteroatoms (H, O, S, N, etc.), was estimated on the base of OC concentrations multiplied by a factor of 1.6, as proposed for urban environments (Putaud *et al.*, 2004). The OM/OC ratio is still a matter of discussion in recent atmospheric studies. Previous observations showed already a wide possible range for the OM/OC ratio, between 1.4-2.1 depending on the

aerosol type (Sandrini *et al*., 2014; Turpin and Lim, 2001). More recent techniques based on the high resolution aerosol mass spectrometry (HR-AMS), which allows the direct measurement of O/C; H/C and N/C ratios confirmed the previous findings reporting the range 1.6-2.1 for Mexico City (Aiken *et al*., 2008) and an average OM/OC of 1.56 for a traffic-related site (Brown *et al*., 2013). The lowest OM/OC ratios are usually seen for fresh combustion aerosols (hydrocarbon-like organic aerosols), while the highest values are usually associated with aged organic aerosols and reflect the presence of oxygenated functional groups formed during atmospheric transport. Higher ratios are indeed observed at background sites or at sites affected by temperature inversion (Malm and Hand, 2007; Turpin and Lim, 2001). Here we use the value of 1.6 as the lower bound of the ratio in areas strongly impacted by primary sources. The OM concentration estimated represents the lower bound of the actual OM. The contribution carbonaceous aerosols and inorganic components was higher in the HS, which can be attributed to the enhanced emissions from residential combustion and traffic (the difference between HS and NHS was statistical significant in terms of T-Test at $p < 0.001$) and meteorological conditions that prevent pollution dispersion (Witkowska *et al*., 2016; Zimnoch *et al*., 2020). OC was dominant in both seasons-18% in the NHS and 34% in the HS. EC mass ranged between 5% in the NHS up to 8% in the HS.

Ionic balance (expressed as ratio of equivalent concentrations of anions to cations) was calculated to check for any indication that not all ions were covered by the direct analysis. During the HS and NHS the ionic balance values were 1.1 and 1.2, respectively. Nitrates, sulfates and ammonium ions, forming the secondary inorganic aerosols (SIA), dominated the inorganic

components in PM_{10} aerosols collected in Wadowice. SIA accounted for 18% of PM_{10} mass in NHS and 21% in HS. NaCl-calculated based on either Na^+ or Cl^-, depending which of those species were less in the equivalent concentration, contributed on average to 2% in NHS and 6% in HS. Chlorine containing compounds can be emitted during coal combustion (McCulloch *et al*., 1999) and it cannot be excluded that the observed chloride originated from coal combustion. In previous studies conducted in Krakow an excess of Cl^- ions in comparison to the equivalent Na^+ concentration was found during the heating season (Junninen *et al*., 2009; Styszko *et al*., 2015). In addition, it was seen that the concentration of the excess Cl^- ions correlated with particulate Mercury, which was a hint for the coal-burning origin. In this study the excess of chloride was observed only in nine samples, mainly those collected in the HS. The amount of chloride not neutralized by Na^+ ranged between 0.4 and 9.6 µg m^{-3}. The highest concentration was very far from the average (2.8 µg m^{-3}) and was noted during the NHS (September), pointing rather to a single local event. If this high value is excluded, a positive correlation ($R^2 = 0.66$) between the excess of Cl^- and PM_{10} concentration can be observed. The small number of samples with this phenomenon does not allow the recognition of other significant relations.

Not identified PM_{10} fraction might include other than analyzed inorganic ions and trace metals, as well as oxygen atoms from their oxides. Moreover, a certain amount of water associate with hygroscopic components (mainly salts) should be accounted. The further part might originate from underestimation of organic matter, derived from the assumed OM/OC ratio.. Based on mineral dust and ions analysis, certain seasonality can be expected also for the missing categories.

Aerosol bound water will be more relevant during HS, as considerably more ions were found during this time. Oxygen atoms will play a significant role (on the relative scale) during NHS, as the mineral fraction was higher during that time. Not identified fraction was 12% and 19% for HS and NHS, respectively. It is similar to values reported elsewhere (Hueglin *et al*., 2005), the average sum for those components was around 19%.

Particulate matter sources

Chemical groups presented in mass closure can be originating from mixed sources. Therefore, the trends of a few source characteristic chemical tracers have been analyzed.

The variability of ratios of organic carbon to elemental carbon (OC/EC) reflects different carbon sources and atmospheric processing. Elemental carbon is mainly emitted from incomplete combustion of fossil fuels, biomass burning and other carbon containing materials. Because organic carbon can originate from fresh emissions (described as primary organic carbon), as well as can be formed through photochemical activity involving gaseous or liquid phase precursors (described as secondary organic carbon)-we analyzed the OC/EC ratio. According to literature (Ji *et al*., 2016; Liu *et al*., 2016; Samara *et al*., 2014; Sillanpää *et al*., 2006), a low OC/EC ratio can be related with fresh sources of traffic aerosol (2.2 and 0.8 for light-duty gasoline and heavy-duty diesel vehicles, respectively) (Na *et al*., 2004; Pio *et al*., 2011; Samara *et al*., 2014), while higher ratios are rather expected for heating sources (coal combustion: 2.6-6.0; wood combustion: 4.15; natural gas: 12.7), forest fires (14.5), dust from paved roads (13.1) (Na *et al*., 2004), and secondary organic carbon (winter-17% of total OC, summer-65% OC (Na *et al*., 2004)). During this study the

322 average OC/EC ratios were 3.7 and 3.8 for NHS and HS, respectively. Ranges of OC/EC in both
323 seasons were very close, 2.1-6.5 in NHS and 1.8-6.5 in HS. The relatively high ratios can be
324 explained by the presence of local sources like wood and coal combustion, as well as contribution
325 of secondary organic carbon, especially during the NHS. Previous studies reported similar OC/EC
326 ratios during HS and NHS in areas affected by wood burning during the cold season (Cao *et al*.,
327 2007; Samek *et al*., 2020, 2017; Sandrini *et al*., 2014; Viana *et al*., 2006). Similarly, Cao *et al*.,
328 (2007) observed similar OC/EC ratios in summer and winter (average about 4) in areas impacted
329 by coal combustion emissions. Ranges of OC/EC in both seasons were very close, 2.1-6.5 in NHS
330 and 1.8-6.5 in HS. The variations of OC/EC obtained for each sample show that local combustion
331 sources are most relevant for the investigated urban area. High correlations (R^2 from 0.685 in NHS
332 to 0.712 in HS) were observed (Fig. 4).
333 The mass ratio of sulfate to nitrate has been used as an indicator of the relative importance of
334 stationary vs. mobile sources of sulfur and nitrogen in the atmosphere. The equivalent ratios of
335 sulfate to nitrate were 5.7 in NHS and 3.7 in HS; therefore, the stationary source emissions,
336 particularly coal burning, were important for SIA formation in these area (Xiu *et al*., 2005). In
337 addition during the HS we observed high relative humidity and low temperature, which favored
338 sulfate formation in the heterogeneous phase through cloud processing. Much lower concentration
339 of NO_3^- during NHS could be driven by the equilibrium between nitrate and nitric acid moved to
340 gas phase due to higher temperatures. The high concentrations of SO_4^{2-} during sampling period,
341 average above 5 µg m^{-3} in HS and NHS (see Table 3) is caused by the coal combustion through

342 whole year for residential, water heating and industry (power station) (Baykara *et al*., 2019;
343 Błaszczak *et al*., 2020; Dai *et al*., 2019; Kozáková *et al*., 2018).

344 ***Concentration trends and distribution of PAHs and 135TPB in PM_{10}***

345 The monthly variations in the total PAHs, 135TPB and PM_{10} mean concentrations, plotted in
346 Fig. 5. shows a strong variability of the target compounds throughout the sampling period. As was
347 expected, the highest concentrations were observed in the HS.

348 The total concentration of the PAHs followed closely the 135TPB concentration, throughout
349 the sampling period. Table 3 provides monthly minimum, average and maximum concentrations of
350 PAHs and 135TPB analyzed in collected samples from February to October 2017. Concentrations
351 of determined PAHs varied from 0.08 ng m^{-3} to 25 ng m^{-3} in whole sampling period and average
352 value of 1 ng m^{-3} in NHS and average value 3.6 ng m^{-3} in HS. The more volatile Naphthalene was
353 not detected, because it is mostly partitioned into the gas phase. The concentration of 135TPB
354 varied from 0.3 ng m^{-3} to 2.6 ng m^{-3}. The average concentration of 135TPB in NHS was 0.3 ng m^{-3}
355 and 0.8 ng m^{-3} in HS.

356 For both periods the heavier 4 and 5 ring PAHs accounted for almost 80% (90% for 11 PAHs
357 in Siudek and Frankowski (2018)) of the total amount of PAHs. The lighter PAHs (3 rings)
358 contribution was up to 7% (6% for 11 PAHs in Siudek and Frankowski (2018),due to extensively
359 partitioning in the atmosphere between the gas and particulate matter Fig. 6.

360 Fig. 7 shows the changes in the mean concentrations of PAHs and 135TPB during heating and
361 non-heating seasons. Only benzo[ghi]perylene's concentrations are similar or higher in the NHS

362 than in the HS (Fig. 7). A relationship profile was created between the concentrations of all PAHs
363 and 135TPB relative to the Pearson coefficient. This coefficient takes values from -1 to 1,
364 respectively: < 0.2-no linear relationship, 0.2-0.4-weak relationship, 0.4-0.7-moderate relationship,
365 0.7-0.9-strong relationship, > 0.9-very strong relationship. The values of the coefficient for PAHs
366 are shown in Table 4, with the exception of compounds that were not present in some months. The
367 highest relationship (the highest value of Pearson coefficient) was observed for fluorene (0.96),
368 indeno[1,2,3-cd]pyrene (0.89) and benzo[k]fluoranthene (0.86).

369 According to Simoneit (2015) 135TPB was found in both types of plastic materials that had
370 been analyzed. Studies have concluded that PAHs, 135TPB and other unknown compounds are
371 derived from PET combustion (Tomsej *et al*., 2018). Co-combustion of both plastics with fuels
372 resulted in a higher abundance of fluorene and most of 4-6 ring PAHs, including
373 indeno[1,2,3-cd]pyrene and benzo[k]fluoranthene. The same relationship between fluorene and
374 135TPB (Pearson 0.96-very strong relationship) was observed in our studies carried out in
375 Wadowice area, where the main sources of pollution are transportation and residential heating. The
376 presence of 135TPB in analysed samples confirms the assumption that plastic waste is burned in
377 the studied area together with other fuels. Due to this fact,135TPB can be used as a good PET
378 combustion marker in air quality monitoring programs.

379 Fig. 8. shows the dependence of 135TPB concentration on temperature. Increased
380 concentrations of 135TPB were noted for lower temperatures (the trends are the same as for PM10
381 yearly concentration-higher particulate matter concentrations at low temperatures promote higher

sorption of compounds), which may confirm that in densely populated areas, plastics are co-burned with fuels in residential furnaces. On the other hand, the higher velocity of wind speed contributed to the decrease in 135TPB concentration regardless of wind direction, Fig. 9. The analysis did not take into account the non-heating period due to many days when 135TPB was below detection limit.

Diagnostic ratios

Ambient concentration of specific air pollutants depend on their emission sources. Those pollutants that are sufficiently stable in the atmosphere and are associated to one source can be used as tracers of that specific source. For example, PHE, FLU and PYR are tracer of coal combustion, BaP and FLU are emitted during wood combustion, whereas FLU, PYR, BbF and BkF are characteristic for diesel engines exhausts. Diagnostic ratios (DR) are ratio between tracers' concentrations. Although diagnostic ratios should be used with caution (Galarneau at al. 2008), their analyses give insights into the identification of particulate matter sources and their relative contribution (e.g. diesel/gasoline engine exhaust gases, biomass/wood/coal combustion) (Yunker *et al*., 2002). Table 5 presents characteristic DRs from various sources (Finardi *et al*., 2017; Kulshrestha *et al*., 2019).

Table 6 summarises the results obtained for the DRs within this study. The analysis assumes the threshold of 50% as an indicator of the effective determination of the source of pollution. In Table 6, only the ratio of FLU/(FLU + PYR), FLT/(FLT + PYR), BaP/(BaP + CH) and BaA/(BaA

402 + CH) can be taken into account because their percentage ratios represent more than the set
403 threshold.

404 The ratio of FLU/(FLU + PYR) indicates petrol combustion as an air pollution source for all
405 measured days in every month taken into consideration. From the FLT/(FLT + PYR) ratio the
406 sources were identified mostly as a fuel combustion. It is worth to note that similar observations for
407 FLT/(FLT + PYR) were reported in other studies (Simoneit, 2015) for areas mainly characterized
408 by the intense transport activities (cars, motorcycles, etc.) and the cities households were mainly
409 heated using wood or coal (Kulshrestha *et al*., 2019). The BaP/(BaP + CH) ratio is used to identify
410 gasoline and diesel combustion. In addition, at residential area during the heating season it allows
411 the identification of firewood and oil from heating radiators as a source of pollution (Manoli *et al*.,
412 2004). BaP/(BaP + CH) in this study indicates the dominance of household heating pollution
413 sources in the winter. In non-heating period sources from road transport dominated. Values of
414 BaA/(BaA + CH) indicates that sources of pollution include vehicles transport (Alves *et al*., 2017).
415 Other authors reported discordant values, e.g. 0.5 for diesel vehicles and 0.73 for gasoline
416 combustion (Finardi *et al*., 2017; Khalili *et al*., 1995). BaP/(BaP + CH) has been considered as
417 household heating pollution sources in the winter and road transport in non-heating period.
418 However, the IP/(IP + BghiP) ratio was not taken into account due to the low percentage of days on
419 which the value of the ratio overlapped the numbers presented in Table 5.

420 DahA came out more often in lower concentrations than BghiP and ideno[1,2,3-cd]pyrene, but
421 the DahA concentration values are much higher during the days when transport dominates (which

422 was also confirmed in this work in Table 6). An example of this is the work of Kozielska *et al*.,
423 (2015) as well as Siudek and Frankowski (2018) where the DahA values exceed the concentrations
424 of BghiP and indeno[1,2,3-cd]pyrene (studies conducted also for Poland-Katowice, Złoty Potok,
425 Poznań).

426 To investigate the impact of long range transported emissions on Wadowice, and especially
427 industrial emissions from Krakow, we analysed air back-trajectory using the Hybrid
428 Single-Particle Lagrangian Integrated Trajectory model (HYSPLIT), developed by NOAA's Air
429 Resources Laboratory. The created pollution transport maps Fig. 10 show the possible trajectory
430 and directions of inflow air masses (8 h backwards, height AGL: 100 m (red line), 300 m (blue line),
431 500 m (green line),).

432 Fig. 10 reports back trajectories calculated for the days when the highest PM_{10} concentrations
433 were recorded over the entire measurement period during the HS (95.0 µg m^{-3} on 09.03.17, Fig. 10.
434 A, 116.8 µg m^{-3} on 13.03.17, Fig. 10. B, 101.5 µg m^{-3} on 27.03.17, Fig. 10. C, 61.4 µg m^{-3} on
435 05.04.17, Fig. 10. D, 60.0 µg m^{-3} on 21.04.17, Fig. 10. E) and NHS (45.3 µg m^{-3} on 01.06.17, Fig.
436 10. F, 33.3 µg m^{-3} on 25.08.17, Fig. 10. G, 107.3 µg m^{-3} on 20.09.17, Fig. 10. H). The maps indicate
437 mostly W, NW, SW and N directions of pollution inflow. NE (Fig. 10. B) wind directions can
438 possibly bring pollution masses from Krakow-the nearest biggest city (over 771,000 citizens).
439 Krakow is located in a basin stretching in the Vistula Valley. In locations of this type, pollution
440 sources are very often concentrated in the city centre, and the long-term movement of air masses
441 leads to its transport to other areas. Examples of PM_{10} emissions sources from the N direction are

coal-fired power plant (Siersza), refinery (Trzebinia) and metallurgical factories (Bukowno, Bolesław, Olkusz) located on the pollution transport route shown in the above graphs. An additional aspect affecting the air quality are domestic furnaces used in transport areas, where solid and high-quality fuels can be burned, as well as waste not intended for this type of furnace. Trajectories from SW/W/NW can be affected by emissions from industrial areas located in Silesia. In fact, this region is well known for many hard coal mines and high density of population. Analyzes of archival data (Environmental Protection Inspectorate in Krakow and Katowice) regarding PM_{10} concentration in backward trajectory areas, show that high concentrations of PM_{10} on a particular day in Wadowice coincided with high PM_{10} concentrations appearing in trajectory areas up to 24 h earlier.

The possible trajectory and directions of inflow of 135TPB were presented below (Fig. 11).

135TPB trajectory analysis in Fig. 11 shows the days with the highest concentration of the plastic burning marker: 1.9 ng m^{-3} 04.04.17 (Fig. 11. A), 2.0 ng m^{-3} on 09.04.17 (Fig. 11. B), 2.2 ng m^{-3} 10.04.17 (Fig. 11. C), 2.3 ng m^{-3} on 01.10.17 (Fig. 11. D), 2.6 ng m^{-3} on 16.10.17 (Fig. 11. E). The maps show mainly the SW direction, which is an area with high population density, characterized by very high air pollution (Bielsko Biała, Szczyrk, Żywiec). However, the NE wind direction is also possible (see Fig. 11. A)-these regions are well know from aircraft industry and furniture factories (Mielec) and chemical industry (Tarnow).

Health risk assessment

From a perspective of human health, the total concentrations of benzo[a]pyrene was above the recommended guideline concentrations of 1 ng m^{-3} (DIRECTIVE 2004/107/EC). The relative impact of the PAH mixture on human health can be determined by different types of indicators such as the carcinogenic equivalent (CEQ), mutagenic equivalent (MEQ), and toxic equivalent (TEQ) (Kozielska *et al*., 2015). The results for analysed months are presented in Table 7. whereas the patterns *(1)-(3*) for the calculations of MEQ, CEQ, TEQ are shown below:

MEQ = 0.00056 * [Acy] + 0.082 * [BaA] + 0.017 * [Chry] + 0.25 * [BbF] + 0.11 * [BkF] + 1 * [BaP] + 0.31 * [IP] + 0.29 * [DahA] + 0.19 * [BghiP] *(1)*

CEQ = 0,001 * ([Nap] + [Acn] + [Acy] + [Flu] + [Phen] + [Flt] + [Pyr]) + 0,01 * ([Ant] + [Chry] + [GghiP]) + 0,1 * ([BaA] + [BbF] + [BkF] + [IP]) + 1 * [BaP] + 5 * [DahA] *(2)*

TEQ = 0.000025 * [BaA] + 0.00020 * [Chry] + 0.000354 * [BaP] + 0.00110 * [IP] + 0.00203 * [DahA] + 0.00253 * [BbF] + 0.00487 * [BkF] *(3)*

Compare to Kozielska *et al*. (Kozielska *et al*., 2015) data, the results obtained in Wadowice presented in this article can be classified as alarmingly high against the background of Europe. For instance, the results obtained for winter 2009 in Madrid (Spain) (Mirante *et al*., 2013) in the urban background are significantly lower than winter months measurements in Wadowice: 0.11 ng m^{-3}, 0.12 ng m^{-3}, 0 ng m^{-3} (for MEQ, CEQ and TEQ, respectively). Going further, to the results from Florence (urban background, Italy) (Martellini *et al*., 2012) in the cold season 2009-2010 were

lower than in summertime in Wadowice: 2.17 ng m^{-3}, 5.43 ng m^{-3}, 0.02 ng m^{-3} (for MEQ, CEQ and TEQ, respectively). Among previously investigated cities in Europe, higher equivalent levels were obtained in winter 2010 in Brno (Czech Republic) (Křůmal *et al*., 2013): 5.85 ng m^{-3}, 8.71 ng m^{-3} and 0.02 ng m^{-3} (for MEQ, CEQ and TEQ, respectively), although they are still significantly lower than results presented for winter period in Wadowice. There are no strictly defined standards for MEQ, CEQ and TEQ values. That coefficients are used for comparison reasons only. However, these values should be as low as possible.

CONCLUSION

This work presents a detailed chemical characterization of PM_{10} in Wadowice duringperiod of 9 months. As sampling was not performed during November to January even higher concentration values might occur during these winter months. The analyzes showed higher concentrations of PM_{10}, PAHs, OC, EC and ions in the colder measurement period than in the warm one. The highest concentrations of particulate matter were recorded on the days when the wind was mostly from W, NW, SW and N directions of pollution inflow. Trajectory analysis suggests seasonal inflow of pollution from industrial areas of Poland. Other pollution sources impacting the measurement area include road transport, coal burning, fuel combustion, smelters. In the case of carbon analysis, organic carbon accounted for the largest fraction of PM_{10} massAs stated in this work, OC may contain polycyclic aromatic hydrocarbons (PAHs) and other organic constituents that have

potential mutagenic, teratogenic and carcinogenic effects. The method used for PAHs analysis did not allow to estimate the concentration for anthracene and naphthalene, due to the low concentration of these compounds in the particle-phase. Nevertheless, larger PAHs were determined and showed elevated concentrations. Strong correlation between PM_{10}, PAHs and emerging contaminants (135TPB) has been noted. The highest relationship (the highest value of Pearson coefficient) was observed between 135TPB and fluorene (0.96). 135TPB is considered as a PET plastic waste incineration marker. The implementation of this type of markers into the atmospheric air monitoring program can help in estimating the contribution of PET combustion in furnaces not adapted for the disposal of plastic waste. Analysis of emerging contaminants is useful tool for identifying sources of pollution, their elimination and air composition control. Health risk assessment showed that mutagenic, carcinogenic, and toxic equivalent (MEQ, CEQ, TEQ), calculated based on PAHs concentrations, are significantly higher than the values observed in other European urban areas. High MEQ, TEQ and CEQ values indicate a high content of carcinogenic compounds, which are a serious problem for human health and life. Purposive actions should be taken immediately to reduce the concentrations of harmful compounds in the atmosphere, and above all to eliminate sources of pollution.

ACKNOWLEDGEMENTS

This research was partially financed by the AGH UST grant 16.16.210.476 subsidy of the Ministry of Science and Higher Education. This work was partially funded by the Rector's Grant for the RedoX Students' Research Group No.AGH90/ Grant/2019. This article is based upon work

522 from COST Action COLOSSAL (CA16109) supported by COST (European Cooperation in
523 Science and Technology). The infrastructure of the AGH Center of Energy in Kraków was applied
524 in order to determine the concentration of ions. Authors thank Krakow Smog Alert for the help in
525 the collection of samples. PF and AS have been partly supported by the EU Project
526 POWR.03.02.00-00-I004/16.

527

528

529

530 # REFERENCES

531 Aiken, A.C., Decarlo, P.F., Kroll, J.H., Worsnop, D.R., Huffman, J.A., Docherty, K.S., Ulbrich,
532 I.M., Mohr, C., Kimmel, J.R., Sueper, D., Sun, Y., Zhang, Q., Trimborn, A., Northway, M.,
533 Ziemann, P.J., Canagaratna, M.R., Onasch, T.B., Alfarra, M.R., Prevot, A.S.H., Dommen, J.,
534 Duplissy, J., Metzger, A., Baltensperger, U. and Jimenez, J.L. (2008). O/C and OM/OC ratios
535 of primary, secondary, and ambient organic aerosols with high-resolution time-of-flight
536 aerosol mass spectrometry. *Environ. Sci. Technol.* 42: 4478–4485.

537 Alves, C.A., Vicente, A.M., Custódio, D., Cerqueira, M., Nunes, T., Pio, C., Lucarelli, F., Calzolai,
538 G., Nava, S., Diapouli, E., Eleftheriadis, K., Querol, X. and Musa, B.A. (2017). Polycyclic
539 aromatic hydrocarbons and their derivatives (nitro-PAHs , oxygenated PAHs, and azaarenes)

in $PM_{2.5}$ from Southern European cities. *Sci. Total Environ.* 595: 494–504.

Baykara, M., Im, U. and Unal, A. (2019). Evaluation of impact of residential heating on air quality of megacity Istanbul by CMAQ. *Sci. Total Environ.* 651: 1688–1697.

Błaszczak, B., Zioła, N., Mathews, B., Klejnowski, K. and Słaby, K. (2020). The Role of $PM_{2.5}$ Chemical Composition and Meteorology during High Pollution Periods at a Suburban Background Station in Southern Poland. *Aerosol Air Qual. Res.* 1: 1–38.

Brown, S.G., Lee, T., Roberts, P.T. and Collett, J.L. (2013). Variations in the OM/OC ratio of urban organic aerosol next to a major roadway. *J Air Waste Manag Assoc.* 63: 1422–1433.

Cao, J., Lee, S.C., Chow, J.C., Watson, J.G., Ho, K.F., Zhang, R.J., Jin, Z.D., Shen, Z.X., Chen, G.C., Kang, Y.M., Zhou, S.C., Zhang, L.Z., Qi, S.H., Dai, M.H., Cheng, Y. and Hu, K. (2007). Spatial and seasonal distributions of carbonaceous aerosols over China. *J. Geophys. Res.* 112: 1–9.

Cavalli, F., Viana, M., Yttri, K.E., Genberg, J. and Putaud, J.P. (2010). Toward a standardised thermal-optical protocol for measuring atmospheric organic and elemental carbon: The EUSAAR protocol. *Atmos. Meas. Tech.* 3: 79–89.

Ciecierska, M. and Obiedziński, M. (2012). Polycyclic aromatic hydrocarbons content in smoked meat products determined by GC-MS method. *Bromatologia i Chemia Toksykologiczna* XLV, 402–407.

558 Dai, Q., Bi, X., Song, W., Li, T., Liu, B., Ding, J., Xu, J., Song, C., Yang, N., Schulze, B.C., Zhang,
559 Y., Feng, Y. and Hopke, P.K. (2019). Residential coal combustion as a source of primary
560 sulfate in Xi'an, China. *Atmos. Environ.* 196: 66–76.

561 Directive 2004/107/EC of the European Parliament and of the Council of 15 December 2004
562 relating to arsenic, cadmium, mercury, nickel and polycyclic aromatic hydrocarbons in
563 ambient air.

564 EPA United States Environmental Protection Agency, List of PAHs recommended for analytical
565 measurement to quantify "Total PAHs", U.S. EPA 2003.

566 Finardi, S., Radice, P., Cecinato, A., Gariazzo, C., Gherardi, M. and Romagnoli, P. (2017).
567 Seasonal variation of PAHs concentration and source attribution through diagnostic ratios
568 analysis. *Urban Clim.* 22: 19–34.

569 Furman, P., Styszko, K., Skiba, A., Durak, J. and Kozioł, W. (2019). Occurrence of PAHs and
570 emerging contaminants, 1,3,5-triphenylbenzene in particulate matter PM_{10} collected in
571 Wadowice. *Abstract book: Ochrona środowiska – rozwiązania i perspektywy : ogólnopolska*
572 *konferencja naukowa*. 44-45.

573 Furman, P., Styszko, K., Skiba, A., Kistler, M., Kasper-Giebl, A. and Zięba, D. (2019). Occurrence
574 of PAHs and new tracer of polyethylene plastic combustion, 1,3,5-triphenylbenzene im PM_{10}
575 collected in residential area of Krakow agglomeration, South Poland. *Abstract book: 12th*
576 *International Conference on Carbonaceous Particles in the Atmosphere (ICCPA) 2019*. 48.

577 Ji, D., Zhang, J., He, J., Wang, X., Pang, B., Liu, Z., Wang, L. and Wang, Y. (2016). Characteristics
578 of atmospheric organic and elemental carbon aerosols in urban Beijing, China. *Atmos.*
579 *Environ.* 125: 293–306.

580 Junninen, H., Mønster, J., Rey, M., Cancelinha, J., Douglas, K., Duane, M., Forcina, V., Müller, A.,
581 Lagler, F., Marelli, L., Borowiak, A., Niedzialek, J., Paradiz, B., Mira-Salama, D., Jimenez, J.,
582 Hansen, U., Astorga, C., Stanczyk, K., Viana, M., Querol, X., Duvall, R.M., Norris, G.A.,
583 Tsakovski, S., Wåhlin, P., Hoŕak, J. and Larsen, B.R. (2009). Quantifying the impact of
584 residential heating on the urban air quality in a typical european coal combustion region.
585 *Environ. Sci. Technol.* 43: 7964–7970.

586 Khalili, N.R., Scheff, P.A. and Holsen, T.M. (1995). PAH source fingerprints for coke ovens,
587 diesel and gasoline engines, highway tunnels, and wood combustion emissions. *Atmos.*
588 *Environ.* 29: 533–542.

589 Kozáková, J., Leoni, C., Klán, M., Hovorka, J., Racek, M., Koštejn, M., Ondráček, J., Moravec, P.
590 and Schwarz, J. (2018). Chemical characterization of $PM_{1\text{-}2.5}$ and its associations with PM_1,
591 $PM_{2.5\text{-}10}$ and meteorology in urban and suburban environments. *Aerosol Air Qual. Res.* 18:
592 1684–1697.

593 Kozielska, B., Rogula-Kozłowska, W. and Klejnowski, K. (2015). Seasonal variations in health
594 hazards from polycyclic aromatic hydrocarbons bound to submicrometer particles at three
595 characteristic sites in the heavily polluted polish region. *Atmosphere* 6: 1–20.

596 Křůmal, K., MikuŠka, P. and Večeřa, Z. (2013). Polycyclic aromatic hydrocarbons and hopanes in
597 PM_1 aerosols in urban areas. *Atmos. Environ.* 67: 27–37.

598 Kubiak, M.S. (2013). Polycyclic Aromatic Hydrocarbons (PAHs) – their occurrence in the
599 environment and food. *Problemy Higieny i Epidemiologii* 94: 31–36.

600 Kulshrestha, M.J., Singh, R. and Ojha, V.N. (2019). Trends and source attribution of PAHs in fine
601 particulate matter at an urban and a rural site in Indo-Gangetic plain. *Urban Clim.* 29: 1–14.

602 Kuskowska, K., Rogula-Kozlowska, W. and Rogula-Kopiec, P. (2018). Particulate matter and
603 polycyclic aromatic hydrocarbons in a selected athletic hall: ambient concentrations, origin
604 and effects on human health. *E3S Web of Conf. Air Protection in Theory and Practice* 28: 1–
605 8.

606 Liu, B., Bi, X., Feng, Y., Dai, Q., Xiao, Z., Li, L., Wu, J., Yuan, J. and Zhang, Y.F. (2016). Fine
607 carbonaceous aerosol characteristics at a megacity during the Chinese Spring Festival as
608 given by OC/EC online measurements. *Atmos. Res.* 181: 20–28.

609 Lochno, A. (2013). *Program ochrony powietrza dla województwa małopolskiego - Małopolska*
610 *2023 - w zdrowej atmosferze*, Kraków.

611 Malm, W.C. and Hand, J.L. (2007). An examination of the physical and optical properties of
612 aerosols collected in the IMPROVE program. *Atmos. Environ.* 41: 3407–3427.

613 Manoli, E., Kouras, A. and Samara, C. (2004). Profile analysis of ambient and source emitted

particle-bound polycyclic aromatic hydrocarbons from three sites in northern Greece. *Chemosphere* 56: 867–878.

Martellini, T., Giannoni, M., Lepri, L., Katsoyiannis, A. and Cincinelli, A. (2012). One year intensive $PM_{2.5}$ bound polycyclic aromatic hydrocarbons monitoring in the area of Tuscany, Italy. Concentrations, source understanding and implications. *Environ. Pollut.* 164: 252–258.

McCulloch, A., Aucott, M.L., Benkovitz, C.M., Graedel, T.E., Kleiman, G., Midgley, P.M. and Li, Y.F. (1999). Global emissions of hydrogen chloride and chloromethane from coal combustion, incineration and industrial activities: Reactive Chlorine Emissions Inventory. *J. Geophys. Res*. 104: 8391–8403.

Mirante, F., Alves, C., Pio, C., Pindado, O., Perez, R., Revuelta, M.A. and Artiñano, B. (2013). Organic composition of size segregated atmospheric particulate matter, during summer and winter sampling campaigns at representative sites in Madrid, Spain. *Atmos. Res.*132–133: 345–361.

Na, K., Sawant, A.A., Song, C. and Cocker, D.R. (2004). Primary and secondary carbonaceous species in the atmosphere of Western Riverside County, California. *Atmos. Environ.* 38: 1345–1355.

Pachurka, Ł., Sówka, I., Fortuna, M. and Zwoździak, A. (2014). Analysis concentration and composition of particulate matter in selected areas of the Lower Silesia Region. *XI Konferencja Naukowa Interdyscyplinarne Zagadnienia w Inżynierii i Ochronie Środowiska*

646–653.

Parol, J., Pietrzak-Fiećko, R. and Smoczyński, S.S. (2014). Polycyclic Aromatic Hydrocarbons (PAHs) in smoked rainbow trout (Oncorhynchus Mykiss). *Food. Science. Technology. Quality* 21: 125–137.

Pio, C., Cerqueira, M., Harrison, R.M., Nunes, T., Mirante, F., Alves, C., Oliveira, C., Sanchez de la Campa, A., Artíñano, B. and Matos, M. (2011). OC/EC ratio observations in Europe: Re-thinking the approach for apportionment between primary and secondary organic carbon. *Atmos. Environ.* 45: 6121–6132.

PN-EN 12341:2006a: Air quality – Determination of the PM_{10} fraction of suspended particulate matter- -reference method and fi eld test procedure to demonstrate reference equivalence of measurement methods.

PN-EN 14907:2006b: Ambient air quality – Standard gravimetric measurement method for the determination of the $PM_{2.5}$ mass fraction of suspended particular matter.

Putaud, J.P., Van Dingenen, R., Alastuey, A., Bauer, H., Birmili, W., Cyrys, J., Flentje, H., Fuzzi, S., Gehrig, R., Hansson, H.C., Harrison, R.M., Herrmann, H., Hitzenberger, R., Hüglin, C., Jones, A.M., Kasper-Giebl, A., Kiss, G., Kousa, A., Kuhlbusch, T.A.J., Löschau, G., Maenhaut, W., Molnar, A., Moreno, T., Pekkanen, J., Perrino, C., Pitz, M., Puxbaum, H., Querol, X., Rodriguez, S., Salma, I., Schwarz, J., Smolik, J., Schneider, J., Spindler, G., ten Brink, H., Tursic, J., Viana, M., Wiedensohler, A. and Raes, F. (2010). A European aerosol

652 phenomenology - 3: Physical and chemical characteristics of particulate matter from 60 rural,
653 urban, and kerbside sites across Europe. *Atmos. Environ.* 44: 1308–1320.

654 Putaud, J.P., Van Dingenen, R., Raes, F., Baltensperger, U., Charron, A., Facchini, M.C., Decesari,
655 S., Fuzzi, S., Gehrig, R., Hansson, H.C., Harrison, R.M., Hüglin, C., Jones, A.M., Laj, P.,
656 Lorbeer, G., Maenhaut, W., Palmgren, F., Querol, X., Rodriguez, S., Schneider, J., Ten Brink,
657 H., Tunved, P., Tørseth, K., Wehner, B., Weingartner, E., Wiedensohler, A. and Wåhlin, P.
658 (2004). A European aerosol phenomenology - 1: Physical characteristics of particulate matter
659 at kerbside, urban, rural and background sites in Europe. *Atmos. Environ.* 38: 2561–2577.

660 Querol, X., Alastuey, A., Viana, M., Moreno, T., Reche, C., Minguillón, M.C., Ripoll, A., Pandolfi,
661 M., Amato, F., Karanasiou, A., Pérez, N., Pey, J., Cusack, M., Vázquez, R., Plana, F.,
662 Dall'Osto, M., De La Rosa, J., Sánchez De La Campa, A., Fernández-Camacho, R.,
663 Rodríguez, S., Pio, C., Alados-Arboledas, L., Titos, G., Artiñano, B., Salvador, P., García Dos
664 Santos, S. and Fernández Patier, R. (2013). Variability of carbonaceous aerosols in remote,
665 rural, urban and industrial environments in Spain: Implications for air quality policy. *Atmos.*
666 *Chem. Phys.* 13: 6185–6206.

667 Rogula-Kozłowska, W., Kozielska, B. and Klejnowski, K. (2013). Concentration, origin and health
668 hazard from fine particle-bound PAH at three characteristic sites in Southern Poland. *Bull*
669 *Environ Contam Toxicol* 91: 349–355.

670 Rogula-Kozłowska, W., Kozielska, B., Majewski, G., Rogula-Kopiec, P., Mucha, W. and

Kociszewska, K. (2018). Submicron particle-bound polycyclic aromatic hydrocarbons in the Polish teaching rooms: Concentrations, origin and health hazard. *J. Environ. Sci.* 64: 235–244.

Samara, C., Voutsa, D., Kouras, A., Eleftheriadis, K., Maggos, T., Saraga, D. and Petrakakis, M. (2014). Organic and elemental carbon associated to PM_{10} and $PM_{2.5}$ at urban sites of northern Greece. *Environ. Sci. Pollut. Res.* 21: 1769–1785.

Samek, L., Stegowski, Z., Furman, L., Styszko, K., Szramowiat, K. and Fiedor, J. (2017). Quantitative Assessment of $PM_{2.5}$ Sources and Their Seasonal Variation in Krakow. *Water Air Soil Pollut*. 228.

Samek, L., Stegowski, Z., Styszko, K., Furman, L. and Fiedor, J. (2018). Seasonal contribution of assessed sources to submicron and fine particulate matter in a Central European urban area. *Environ. Pollut* 241: 406–411.

Samek, L., Stegowski, Z., Styszko, K., Furman, L., Zimnoch, M., Skiba, A., Kistler, M., Kasper-Giebl, A., Rozanski, K. and Konduracka, E. (2020). Seasonal variations of chemical composition of $PM_{2.5}$ fraction in the urban area of Krakow, Poland: PMF source attribution. *Air Qual Atmos Health* 13:89-96.

Sandrini, S., Fuzzi, S., Piazzalunga, A., Prati, P., Bonasoni, P., Cavalli, F., Bove, M.C., Calvello, M., Cappelletti, D., Colombi, C., Contini, D., de Gennaro, G., Di Gilio, A., Fermo, P., Ferrero, L., Gianelle, V., Giugliano, M., Ielpo, P., Lonati, G., Marinoni, A., Massabò, D., Molteni, U.,

690 Moroni, B., Pavese, G., Perrino, C., Perrone, M.G., Perrone, M.R., Putaud, J.P., Sargolini, T.,
691 Vecchi, R. and Gilardoni, S. (2014). Spatial and seasonal variability of carbonaceous aerosol
692 across Italy. *Atmos. Environ.* 99: 587–598.

693 Sillanpää, M., Hillamo, R., Saarikoski, S., Frey, A., Pennanen, A., Makkonen, U., Spolnik, Z., Van
694 Grieken, R., Braniš, M., Brunekreef, B., Chalbot, M.C., Kuhlbusch, T., Sunyer, J., Kerminen,
695 V.M., Kulmala, M. and Salonen, R.O. (2006). Chemical composition and mass closure of
696 particulate matter at six urban sites in Europe. *Atmos. Environ.* 40: 212–223.

697 Simoneit, B.R.T. (2015). Triphenylbenzene in Urban Atmospheres, a New PAH Source Tracer.
698 *Polycyclic Aromatic Compounds* 35: 3–15.

699 Simoneit, B.R.T., Kobayashi, M., Mochida, M., Kawamura, K. and Huebert, B.J. (2004). Aerosol
700 particles collected on aircraft flights over the northwestern Pacific region during the
701 ACE-Asia campaign: Composition and major sources of the organic compounds. *J. Geophys.*
702 *Res*. 109: 1–13.

703 Simoneit, B.R.T., Medeiros, P.M. and Didyk, B.M. (2005). Combustion products of plastics as
704 indicators for refuse burning in the atmosphere. *Environ Sci Technol*. 39: 6961–6970.

705 Siudek, P. and Frankowski, M. (2018). The role of sources and atmospheric conditions in the
706 seasonal variability of particulate phase PAHs at the urban site in Central Poland. *Aerosol Air*
707 *Qual Res.* 18: 1405–1418.

708 Skiba, A., Styszko, K., Furman, P., Dobrowolska, N., Kistler, M., Kasper-Giebl, A. and Zięba, D.
709 (2019). Polycyclic aromatic hydrocarbons (PAHs) associated with PM_{10} collected in
710 Wadowice, South Poland. *E3S Web of Conf.* 108: 02007.

711 Styszko, K., Skiba, A., Kasper-Giebl, A., Tobler, A., Casotto, R., Prevot, A.S., Nęcki J. and
712 Różański, K. (2019a). Characterization of carbonaceous species in PM_{10} fraction in Krakow
713 (Southern Poland) during warm and cold season using off-line and on-line instrumentation.
714 *Abstract book: EAC2019 European Aerosol Conference P3-145.*

715 Styszko, K., Skiba, A., Samek, L., Furman, P., Kistler, M., Kasper-Giebl, A., Zimnoch, M.,
716 Różański, K. and Konduracka, E. (2019b). Characteristics of organic compounds in $PM_{2.5}$
717 collected in Krakow, Southern Poland. *Abstract book: EAC2019 European Aerosol*
718 *Conference P2-040.*

719 Styszko, K., Szramowiat, K., Kistler, M., Kasper-Giebl, A., Samek, L., Furman, L., Pacyna, J. and
720 Gołaś, J. (2015). Mercury in atmospheric aerosols: A preliminary case study for the city of
721 Krakow, Poland. *C R Chim.* 18: 1183–1191.

722 Szramowiat, K., Styszko, K., Kistler, M., Kasper-Giebl, A. and Gołas, J. (2016). Carbonaceous
723 species in atmospheric aerosols from the Krakow area (Malopolska District): Carbonaceous
724 species dry deposition analysis. *E3S Web of Conf.* 10: 4–11.

725 Tian, J., Ni, H., Cao, J., Han, Y., Wang, Q., Wang, X., Chen, L.W.A., Chow, J.C., Watson, J.G.,
726 Wei, C., Sun, J., Zhang, T. and Huang, R. (2017). Characteristics of carbonaceous particles

from residential coal combustion and agricultural biomass burning in China. *Atmos. Pollut. Res* 8: 521–527.

Tomsej, T., Horak, J., Tomsejova, S., Krpec, K., Klanova, J., Dej, M. and Hopan, F. (2018). The impact of co-combustion of polyethylene plastics and wood in a small residential boiler on emissions of gaseous pollutants, particulate matter, PAHs and 1,3,5- triphenylbenzene. *Chemosphere* 196: 18–24.

Turpin, B.J. and Lim, H.J. (2001). Species contributions to $PM_{2.5}$ mass concentrations: Revisiting common assumptions for estimating organic mass. *Aerosol Sci Technol.* 35: 602–610.

Viana, M., Chi, X., Maenhaut, W., Querol, X. and Alastuey, A. (2006). Organic and elemental carbon concentrations in carbonaceous aerosols during summer and winter sampling campaigns in Barcelona , Spain. *Atmos. Environ.* 40: 2180–2193.

Witkowska, A., Lewandowska, A.U., Saniewska, D. and Falkowska, L.M. (2016). Effect of agriculture and vegetation on carbonaceous aerosol concentrations ($PM_{2.5}$ and PM_{10}) in Puszcza Borecka National Nature Reserve (Poland). *Air Qual Atmos Health* 9: 761–773.

Xiu, G.L., Jin, Q., Zhang, D., Shi, S., Huang, X., Zhang, W., Bao, L., Gao, P. and Chen, B. (2005). Characterization of size-fractionated particulate mercury in Shanghai ambient air. *Atmos. Environ.* 39: 419–427.

Yunker, M.B., Macdonald, R.W., Vingarzan, R., Mitchell, H., Goyette, D. and Sylvestre, S. (2002).

PAHs in the Fraser River basin : a critical appraisal of PAH ratios as indicators of PAH source and composition. *Org. Geochem.* 33: 489–515.

Zhang, Y., Obrist, D., Zielinska, B. and Gertler, A. (2013). Particulate emissions from different types of biomass burning. *Atmos. Environ.* 72: 27–35.

Zimnoch, M., Samek, L., Furman, L., Styszko, K., Skiba, A., Gorczyca, Z., Galkowski, M., Rozanski, K. and Konduracka, E. (2020). Application of Natural Carbon Isotopes for Emission Source Apportionment of Carbonaceous Particulate Matter in Urban Atmosphere : A Case Study from Krakow, Southern Poland. *Sustainability* 12: 1–9.

Tables

Table 1. Monthly averages, minimal and maximal values of meteorological conditions in sampling period in Wadowice.

Month	Temperature [°C] (min-max)	Precipitation [mm] (min-max)	Pressure [hPa] (min-max)	Wind speed [m s^{-1}] (min-max)	Prevailing wind direction
February	1.5-7.0	0.0-0.0	969-984	3.4-5.0	SW
March	3.0-12.5	0.0-0.0	966-991	1.7-6.7	W/SW
April	1.0-15.5	0.2-22.3	973-991	1.3-6.5	W/N
May	4.5-21.5	0.2-30.6	971-992	1.5-4.1	N
June	14.5-19.5	1.9-7.4	977-986	1.7-4.7	W/N
August	13.5-31.5	0.2-29.3	970-982	0.0-4.1	W
September	9.0-19.5	1.0-57.8	972-988	1.3-5.6	W/E
October	7.5-16.0	0.1-11.8	961-986	1.0-8.1	W

Table 2. Chromatographic and mass spectrometric characterization of target analytes: retention time, mass of characteristic ions and correlation coefficients-R^2.

Compound	Retention time [min]	Precursor-products ions m z^{-1}	R^2	MQL [ng m^{-3}]
Naphthalene	7.08	128-102,	0.9990	6.25
Acenaphthylene	10.15	152-150, 126	0.9999	0.26
Acenaphthene	10.43	153-150, 126	0.9998	0.02
Fluorene	11.50	165-163, 139	0.9997	0.14
Phenathrene	14.03	178-152, 176	0.9991	0.29
Anthracene	14.11	178-152, 176	0.9996	6.25
Fluoranthene	17.08	202-200, 174	0.9989	0.30
Pyrene	17.82	202-200, 174	0.9998	0.12

Benzo(a)anthracene	20.81	228-226, 202	0.9977	0.38
Chrysene	21.03	228-226, 202	0.9995	0.17
Benzo(b)fluoranthene	24.23	252-250, 226	0.9945	0.56
Benzo(k)fluoranthene	24.32	252-250, 226	0.9984	0.17
Benzo(a)pyrene	26.05	252-250, 226	0.9960	0.45
Indeno(1,2,3-cd)pyrene	32.83	276-274, 248	0.9943	0.80
Dibenz(a,h)anthracene	32.84	278-276, 252	0.9941	0.78
Benzo(g,h,i)perylene	35.69	276-274, 248	0.9962	0.50
1,3,5- triphenylbenzene	25.02	306-289, 228	0,9991	0,18
Benzo[a]pyrene-d_{12}	25.88	264-262, 216	-	-

780

781 **Table 3.** Concentrations of analyzed components constituting to mass closure, collected during
782 the heating and non-heating seasons

Concentration	Heating season			Non-heating season		
[µg m^{-3}]	min	max	average	min	max	average
PM_{10}	10.94	116.77	43.30	10.80	53.70	27.12
OC	5.90	39.32	14.46	3.84	20.75	7.66
EC	1.48	6.93	3.70	1.08	4.64	2.11
Na^+	0.00	3.94	2.07	1.15	2.68	1.78
NH_4^+	0.00	5.01	1.40	0.26	2.45	0.92
Mg^{2+}	0.00	1.07	0.37	0.02	1.29	0.21
K^+	0.33	1.00	0.50	0.34	0.88	0.49
Ca^{2+}	0.00	3.20	0.72	0.02	2.63	0.81
NO_3^-	0.62	12.04	2.52	0.53	4.03	1.45
SO_4^{2-}	2.19	13.26	5.58	2.24	11.81	5.35
Cl^-	0.15	9.91	1.86	0.15	11.92	0.57
PAHs [ng m^{-3}]						
Naphthalene	<MQL	<MQL	<MQL	<MQL	<MQL	<MQL
Acenaphthylene	0.26	1.88	0.57	0.27	0.90	0.54
Acenaphthene	0.02	0.11	0.02	0.02	0.03	0.02
Fluorene	0.14	1.23	0.51	0.15	0.57	0.16
Phenathrene	0.42	4.17	1.44	0.30	0.86	0.36
Anthracene	<MQL	<MQL	<MQL	<MQL	<MQL	<MQL
Fluoranthene	1.07	5.52	1.60	0.47	2.19	0.71
Pyrene	0.89	20.49	4.68	0.41	2.24	0.71
Benzo(a)anthracene	1.60	24.73	6.98	0.61	3.43	1.16
Chrysene	1.16	21.52	6.10	0.50	3.23	1.08
Benzo(b)fluoranthene	1.88	19.99	6.90	0.95	3.72	1.63

Benzo(k)fluoranthene	1.32	10.16	3.68	0.54	2.15	0.89
Benzo(a)pyrene	0.49	20.93	4.98	0.64	3.66	1.10
Indeno(1,2,3-cd)pyrene	2.50	14.18	5.86	1.02	3.52	1.61
Dibenz(a,h)anthracene	1.60	20.00	6.24	1.17	3.59	1.43
Benzo(g,h,i)perylene	0.51	9.25	1.82	0.50	3.24	1.27
1,3,5-triphenylbenzene	0.39	2.56	0.83	0.26	0.90	0.30

Table 4. Concentrations of analyzed components constituting to mass closure, collected during the heating and non-heating seasons

PAHs	Pearson	Relationship
Acenaphthylene	0.76	Strong relationship
Benzo[a]anthracene	0.72	Strong relationship
Benzo[a]pyrene	0.67	Moderate relationship
Benzo[b]fluoranthene	0.78	Strong relationship
Bnzo[ghi]perylene	0.55	Moderate relationship
Benzo[k]fluoranthene	0.86	Strong relationship
Chrysene	0.73	Strong relationship
Dibenzo[a,h]anthracene	0.76	Strong relationship
Fluoranthene	0.38	Weak relationship
Fluorene	0.96	Very strong relationship
Indeno[1,2,3-cd]pyrene	0.89	Strong relationship
Phenanthrene	0.82	Strong relationship
Pyrene	0.66	Moderate relationship

795

796

797

798

799

800

801 **Table 5.** Characteristic diagnostic indicators from different sources (Yunker *et al*., 2002; Finardi
802 *et al*., 2017; Kulshrestha *et al*., 2019; Manoli *et al*., 2004; Célia A. Alves *et al*. 2017; Khalili,
803 Scheff and Holsen, 1995; Simoneit, 2015, Galarneau, E. 2008; Taosheng Jin *et al*. 2018)

Ratio	Value range	Source
FLU/(FLU+PYR)	< 0.5	Petrol emission
	> 0.5	Diesel emission
FLT/(FLT+PYR)	< 0.40	Petrogenic emission
	0.40-0.50	Fuel combustion
	> 0.50	Coal, wood burning
BbF/BkF	0.92	Wood burning
	1.26	Vehicles
	2.5-2.9	Smelters
	3.5-3.9	Coal/coke
PYR/BaP	0.9 ± 0.4	Gasoline exhaust
	0.8 ± 0.9	Diesel exhaust
	0.70	Wood combustion
BaP/(BaP+CH)	0.08-0.39	Wood burning
	< 0.50	House heating
	> 0.50	Mobile sources
IcdP/(IcdP+BghiP)	0.18	Car
	0.37	Diesel exhaust
	0.32	Gasoline vehicles
	0.32	Natural gas combustion
	0.36	Oil combustion
	0.56	Coal
	0.64	Wood burning
BaA/(BaA+CH)	0.50	Vehicles
	0.73	Gasoline and diesel exhausts

804

805

806

807

808 **Table 6.** Monthly indicators results.

Ratio	Value range	Source	Months with the number of days %							
			Feb (4)	Mar (27)	Apr (25)	May (25)	Jun (13)	Aug (30)	Sep (14)	Oct (16)
FLU/(FLU+PYR)	< 0.5	Petrol emission	100	100	100	100	100	100	100	100
	> 0.5	Diesel emission	0	0	0	0	0	0	0	0
FLT/(FLT+PYR)	< 0.4	Petrogenic emission	0	100	20	36	38	0	0	0
	0.4-0.5	Fuel combustion	100	0	48	36	0	87	79	88
	> 0.5	Coal and wood burning	0	0	32	28	62	13	21	12
BbF/BkF	0.92	Wood burning	0	0	0	0	0	0	0	0
	1.26	Vehicles	0	0	16	0	62	0	14	0
	2.5-2.9	Smelters	0	0	0	0	0	0	0	0
	3.5-3.9	Coal/coke	0	0	0	0	0	0	0	0
PYR/BaP	0.9 ± 0.4	Gasoline exhaust	0	30	0	0	0	0	0	6
	0.8 ± 0.9	Diesel exhaust	0	33	0	0	0	0	0	0
	0.70	Wood combustion	0	37	0	8	23	10	0	0
BaP/(BaP+CH)	0.08-0.39	Wood burning	100	0	80	0	0	3	86	100
	< 0.50	House heating	100	26	100	36	38	3	86	100
	> 0.50	Mobile sources	0	74	0	64	62	97	14	0
IcdP/(IcdP+BghiP)	0.18	Car	0	0	0	0	0	0	0	0
	0.37	Diesel exhaust	0	0	0	0	0	0	0	0
	0.32	Gasoline vehicles	0	0	0	0	0	0	0	0
	0.32	Natural gas combustion	0	0	0	0	0	0	0	0
	0.36	Oil combustion	0	0	0	0	0	0	0	0
	0.56	Coal	0	0	0	28	28	0	14	19
	0.64	Wood burning	0	0	0	0	23	0	0	44
BaA/(BaA+CH)	0.5	Vehicles	100	100	80	64	62	100	100	100
	0.73	Gasoline & diesel exhausts	0	0	0	0	0	0	0	0

809

Table 7. Monthly mean values of carcinogenic equivalent (CEQ), mutagenic equivalent (MEQ) and toxic equivalent (TEQ).

	Feb	Mar	Apr	May	Jun	Aug	Sep	Oct	Average
MEQ	10.5	22.3	10.7	4.6	3.3	3.1	3.8	5.6	8.0
CEQ	21.3	72.8	27.2	10.2	11.0	13.0	11.5	16.6	23.0
TEQ	0.04	0.1	0.04	0.02	0.01	0.01	0.02	0.04	0.04

Figure Captions

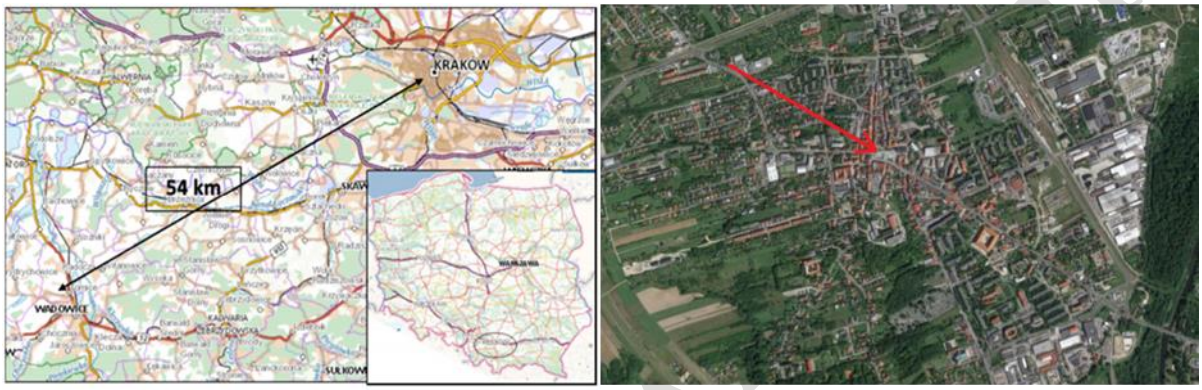

Fig. 1. Maps showing the sampling point location in Wadowice.

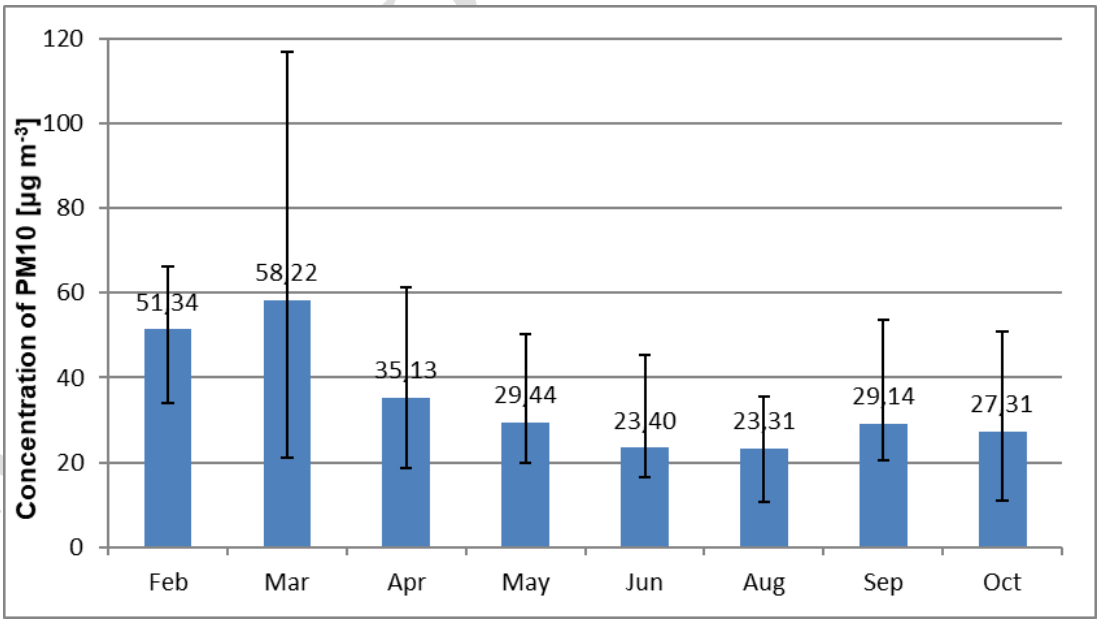

Fig. 2. Time series of monthly average PM_{10} concentrations during the sampling period.

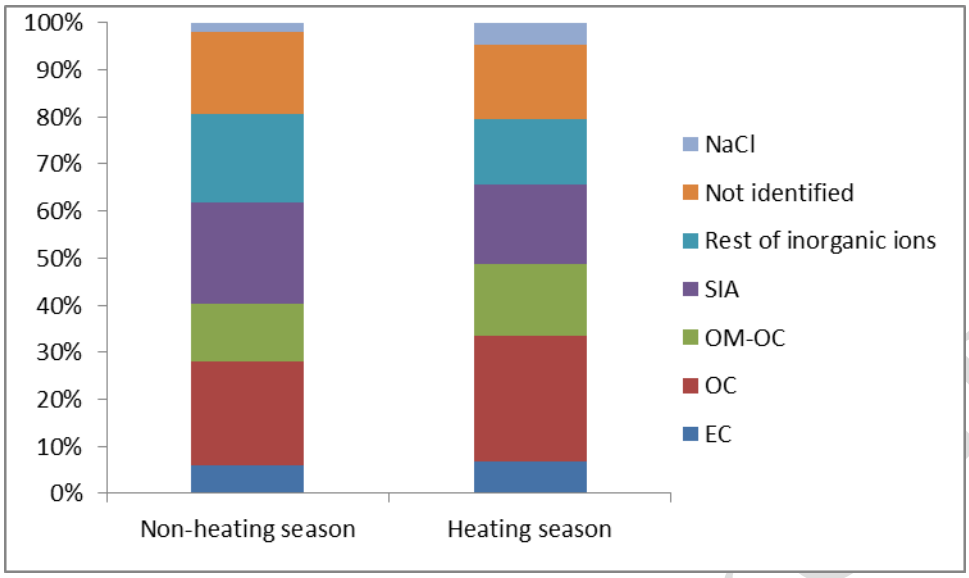

842

843 **Fig. 3.** Average chemical composition of particulate matter for two seasons.

844

845

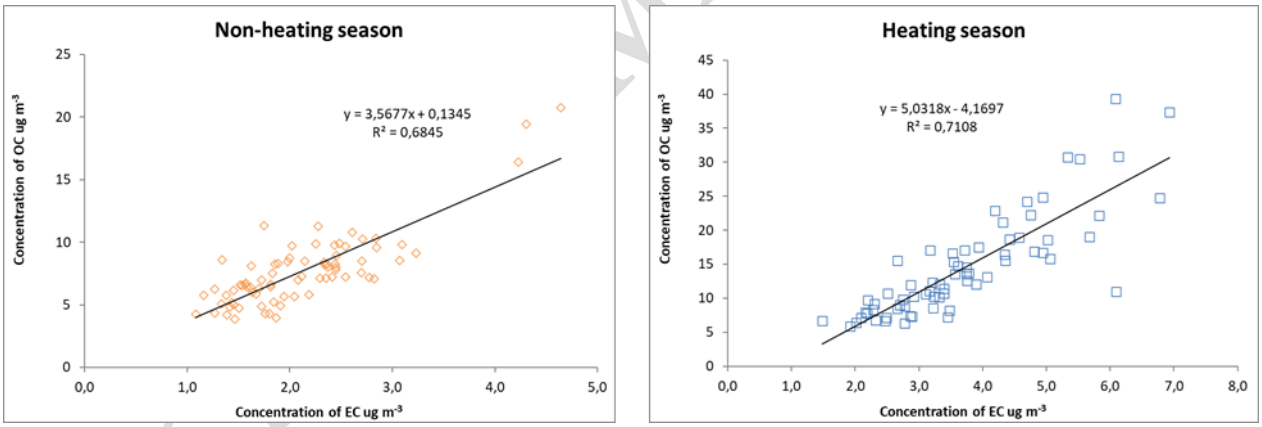

846

847 **Fig. 4.** Scatterplots of OC and EC concentrations and linear regression for two seasons.

848

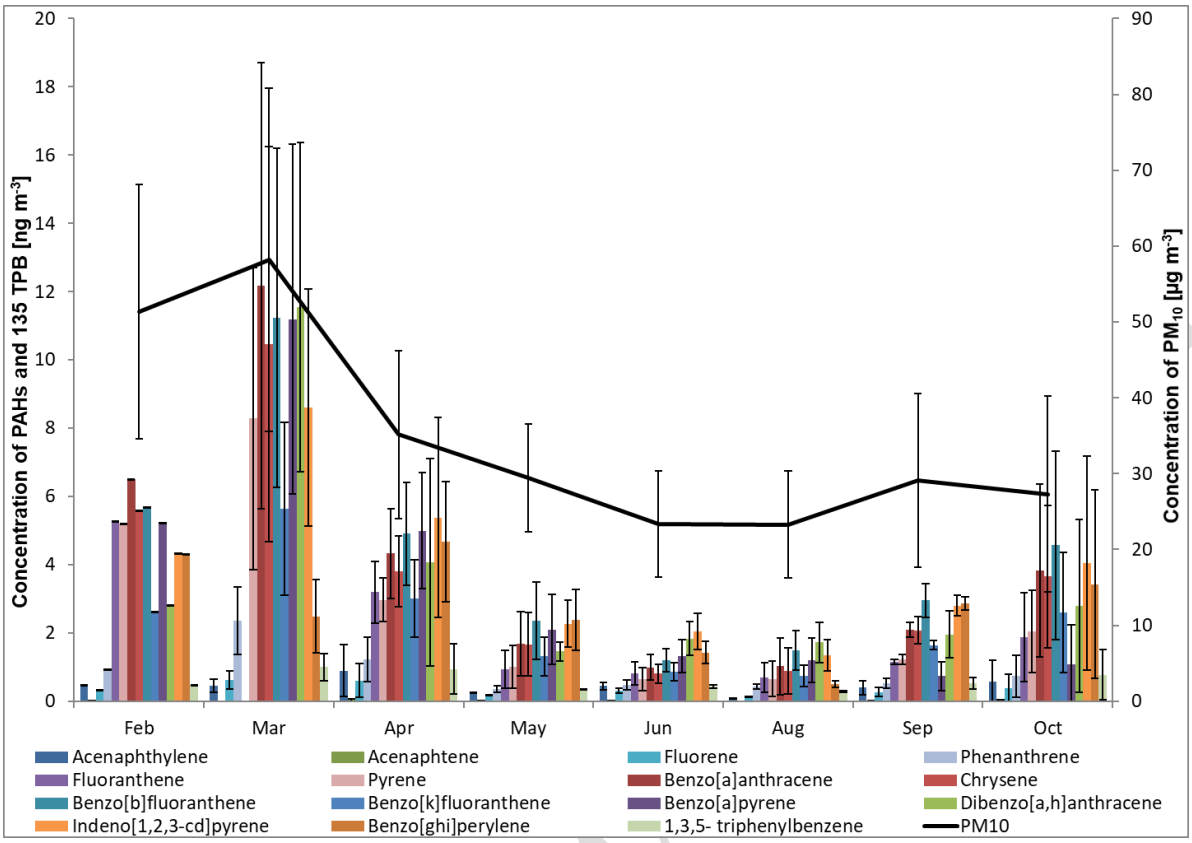

849

850 **Fig. 5**. Variation of the average concentrations of the PAHs and 135TPB throughout the sampling
851 period. Bars represent standard deviations between sampling days.

852

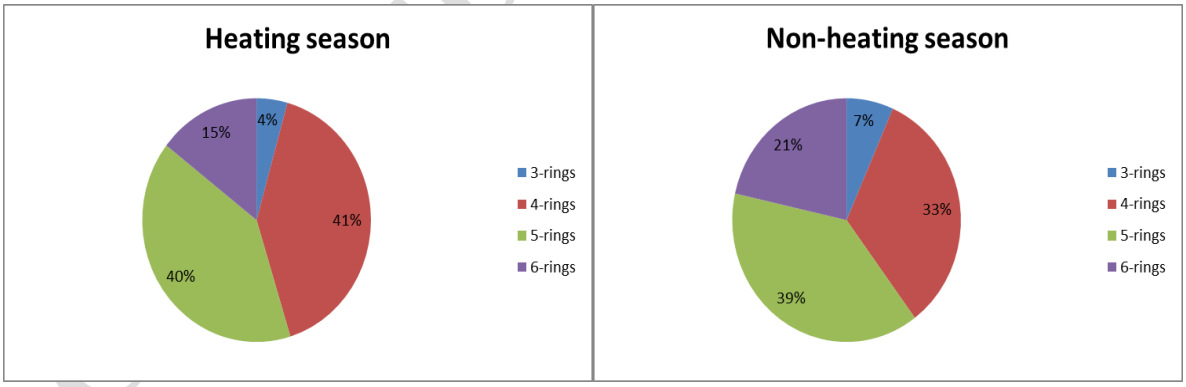

853

854 **Fig. 6.** Ring number distribution of PM_{10} associated PAHs during heating and non-heating seasons.

855

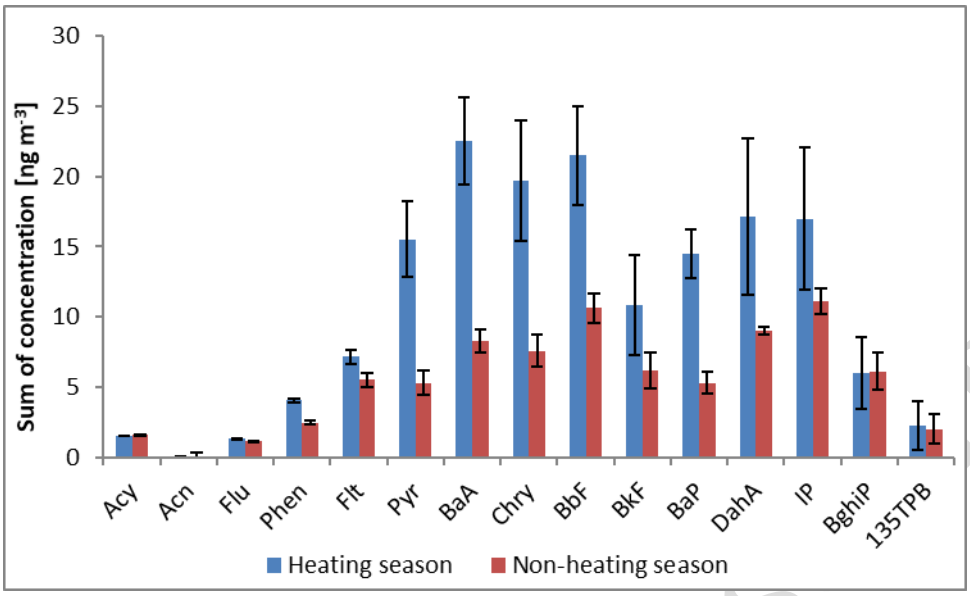

856

857 **Fig. 7.** The mean concentrations of PAHs and 135TPB in heating and non-heating seasons.

858

859

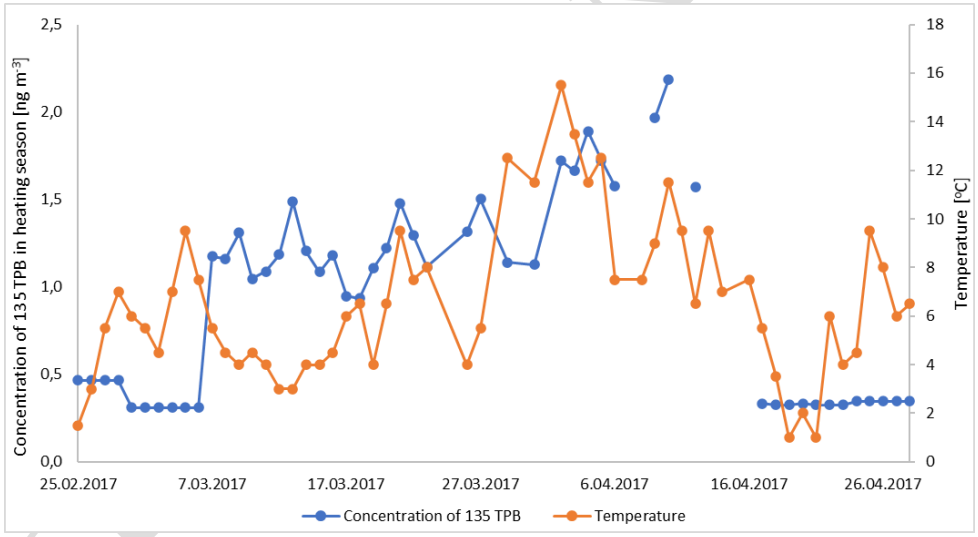

860

861 **Fig. 8.** Trend between concentration of 135TPB and temperature through the heating season (Some
862 days were not presented due to the value of 135TPB below LOQ)

863

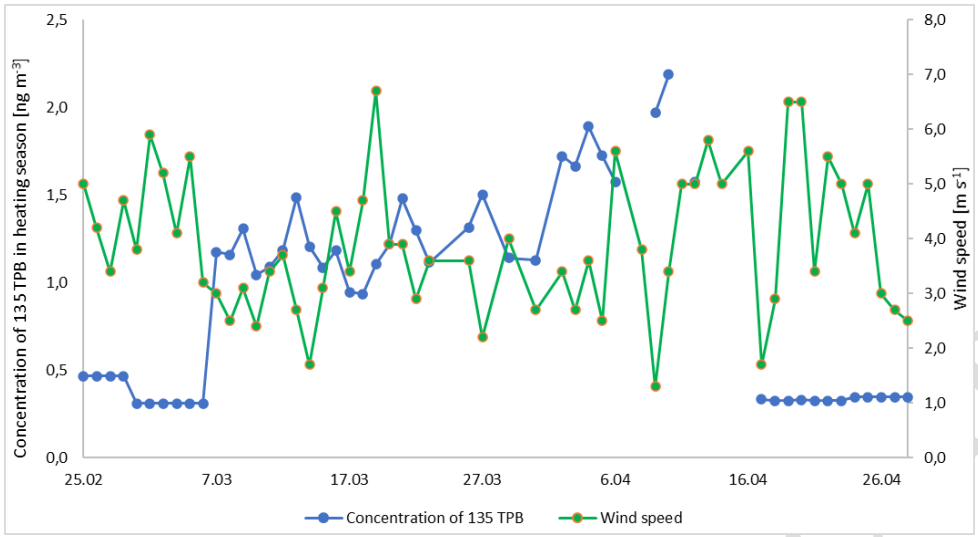

Fig. 9. Trend between concentration of 135TPB and wind speed through the heating season (Some days were not presented due to the value of 135TPB below LOQ)

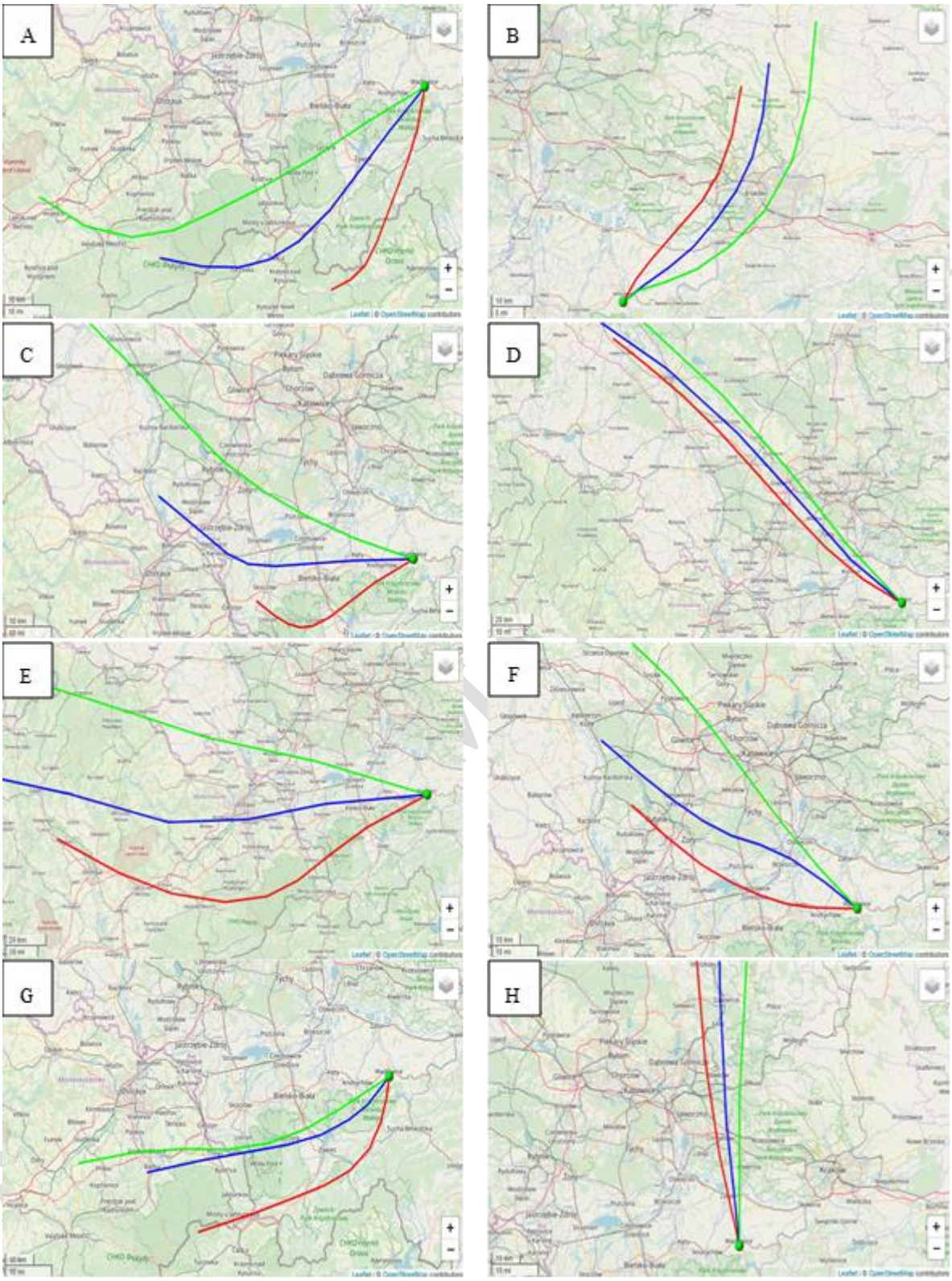

Fig. 10. The air masses trajectory and directions during selected days of the measured period: A-09.03, B-13.03, C-27.03, D-05.04, E-21.04, F-01.06, G-25.08, H-20.09.

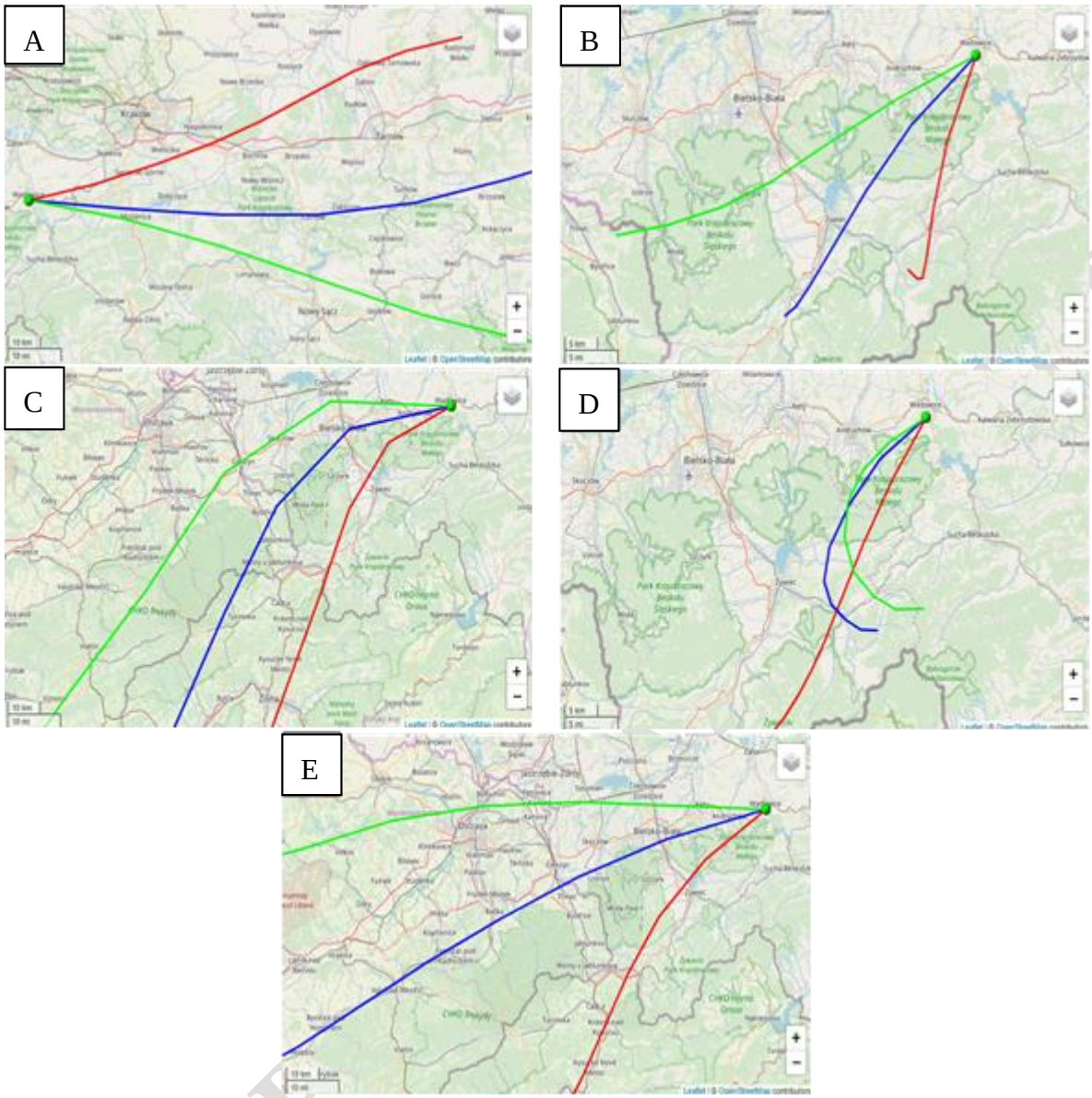

872

873 **Fig. 11.** The 135TPB trajectory and directions during selected days of the measured period:
874 A-04.04, B-09.04, C-10.04, D-01.10, E-16.10.

875